PHYSICAL REVIEW D **93,** 074006 (2016)

Topological susceptibility in three-flavor quark-meson model at finite temperature

Yin Jiang,[1,2] Tao Xia,[1,3] and Pengfei Zhuang[1]

[1]*Physics Department, Tsinghua University and Collaborative Innovation Center of Quantum Matter, Beijing 100084, People's Republic of China*

[2]*Physics Department and Center for Exploration of Energy and Matter, Indiana University, 2401 North Milo B. Sampson Lane, Bloomington, Indiana 47408, USA*

[3]*College of OptoElectronic Science and Engineering, National University of Defense Technology, Changsha 410073, People's Republic of China*

(Received 21 November 2015; revised manuscript received 19 February 2016; published 6 April 2016)

We study $U_A(1)$ symmetry and its relation to chiral symmetry at finite temperature through the application of the functional renormalization group to the $SU(3)$ quark-meson model. Very different from the mass gap and mixing angel between η and η' mesons, which are defined at the mean-field level and behavior like condensates, the topological susceptibility includes a fluctuation-induced part which becomes dominant at high temperature. As a result, the $U_A(1)$ symmetry is still considerably broken in the chiral symmetry restoration phase.

DOI: 10.1103/PhysRevD.93.074006

I. INTRODUCTION

It is well known that the $U_A(1)$ symmetry is broken in the vacuum of quantum chromodynamics (QCD) by the anomaly due to the nontrivial topology of the principal bundle of the gauge field [1,2], which leads to the nondegeneracy of η and η' mesons [3–5]. As a strong interacting system should approach its classic limit at high temperature, all the broken symmetries including the $U_A(1)$ are expected to be restored in a hot medium [6]. While the relation between the $U_A(1)$ symmetry and chiral symmetry in vacuum and at finite temperature has been studied for a long time [7–13], it is still an open question whether the $U_A(1)$ symmetry is restored in the chiral symmetric phase.

The lattice simulation is a powerful tool to study QCD symmetries. By a proper definition, the topological charge and its susceptibility are used to describe the $U_A(1)$ anomaly in the pure gauge field theory and the unquenched theory [14,15]. In both cases, the susceptibility drops above the critical temperature T_c of the chiral restoration, but the charge keeps an obvious deviation from zero at high temperature $T > T_c$. The simulation for the instanton model shows such a partial restoration, too [16]. From the recent lattice simulations of the HotQCD [17] and JLQCD [18] collaborations, while the $U_A(1)$ symmetry is still broken at T_c from both groups, the JLQCD claimed the $U_A(1)$ restoration at $T = 1.2T_c$ and the HotQCD observed the opposite result.

To clearly understand the relation between the $U_A(1)$ and chiral symmetries, we need to put the QCD system in the chiral limit where the chiral phase transition at high temperature is well defined. In a real case with nonzero quark mass, the chiral symmetry cannot be fully restored by thermodynamics, and, therefore, one possible mechanism of the $U_A(1)$ breaking at high temperature is the residual chiral breaking. Since the chiral limit cannot be realized in lattice calculations where a nonzero pion mass is always used, we need to consider effective models to clarify the relation between the two symmetries. Two of the often employed models are the Nambu–Jona-Lasinio (NJL) [19] model at the quark level [20–24] and the linear sigma model at the hadron level [25,26] and including quarks (quark-meson model) [27,28]. At finite temperature and density, the two models are widely used to discuss chiral and $U_A(1)$ properties of strongly interacting matters; see, for instance, [29–39].

In this work, we use the functional renormalization group (FRG) method to study $U_A(1)$ symmetry and its relation to chiral symmetry in the quark-meson model. As a nonperturbative method, the FRG [40,41] has been used to study phase transitions in various systems like cold atom gas [42], nucleon gas [43], and hadron gas [44–49]. By solving the flow equation which connects physics at different momentum scales, the FRG shows great power to describe the phase transitions and the corresponding critical phenomena which are normally difficult to be controlled in the mean-field approximation because of the absence of quantum fluctuations. Instead of adding hot loops to the thermodynamic potential in the usual ways of going beyond the mean field, the fluctuations are included in the FRG effective action through running the RG scale from the ultraviolet limit to the infrared limit, which, as an advantage, can automatically guarantee the Nambu-Goldstone theorem in the symmetry breaking phase. Based on our previous works in the linear sigma [50] and NJL [51] models where we focused on the meson masses, we calculate here in the $SU(3)$ quark-meson model the topological susceptibility and $\eta - \eta'$ mixing angle which describes directly and clearly the degree of $U_A(1)$ symmetry breaking. We will see that while the $U_A(1)$ is controlled by the chiral condensate in the chiral breaking phase, it is dominated by fluctuations after the chiral symmetry is restored.

The paper is organized as follows. In Sec. II we first define in the quark-meson model the correspondent of the topological charge density Q of QCD and then calculate analytically the topological susceptibility χ. In Sec. III we briefly review the FRG application to the quark-meson model and introduce the pseudoscalar meson's mixing angle θ_P. In Sec. IV we numerically solve the FRG flow equations with the grid method and show the temperature dependence of the scalar and pseudoscalar mesons as well as the mixing angle and the topological susceptibility. We summarize in Sec. V.

II. TOPOLOGICAL SUSCEPTIBILITY IN THE $SU(3)$ QUARK-MESON MODEL

The topological susceptibility is a fundamental correlation function in QCD and is the key to understanding the dynamics in the $U_A(1)$ channel. In this section, we calculate the topological susceptibility at finite temperature within the framework of the three-flavor quark-meson model.

In QCD, the axial current $J_5^\mu = \bar{\psi}\gamma^\mu\gamma_5\psi$ is not conserved due to the $U_A(1)$ anomaly induced by the instanton effect,

$$\partial_\mu J_5^\mu = 2N_f Q(x) + 2im_0\bar{\psi}\gamma_5\psi, \tag{1}$$

where m_0 is the current quark mass, $N_f = 3$ the number of flavors, and Q the topological charge density

$$Q(x) = \frac{g^2}{32\pi^2} F^a_{\mu\nu}\tilde{F}^{\mu\nu}_a \tag{2}$$

with the gluon field strength tensor $F^a_{\mu\nu}$ and the coupling constant g between the quark and gluon fields. The topological susceptibility χ is defined as the Fourier transform of the connected correlation function $\langle T(Q(x)Q(0))\rangle$,

$$\chi = \int d^4x \langle T(Q(x)Q(0))\rangle_{\mathrm{connected}}, \tag{3}$$

where T denotes the time-ordering operator.

We now define the correspondent of the topological charge density Q in the three-flavor quark-meson model through the conservation law (1). The Lagrangian density of the model contains the meson section and quark section,

$$\mathcal{L} = \mathcal{L}_m + \mathcal{L}_q. \tag{4}$$

The coupling between the quark and meson fields is included in the quark section. Taking renormalizability into account in Minkowski space, the meson section $\mathcal{L}_m$ reads

$$\begin{aligned}\mathcal{L}_m = {} & \mathrm{Tr}[\partial_\mu\Phi\partial^\mu\Phi^\dagger] - (m^2\rho_1 + \lambda_1\rho_1^2 + \lambda_2\rho_2) \\ & + c\xi + \mathrm{Tr}[H(\Phi+\Phi^\dagger)],\end{aligned} \tag{5}$$

where the meson matrix $\Phi = T^a\phi_a$ and the trace Tr are defined in the flavor space, the meson fields $\phi_a = \sigma_a + i\pi_a$ contain nine scalar mesons σ_a and nine pseudoscalar mesons π_a, the 3×3 Gell-Mann matrices $T_a = \lambda_a/2$ for $a = 1,\ldots,8$ and $T_0 = \mathbf{1}/\sqrt{6}$ for $a = 0$ obeys the relations $\mathrm{Tr}(T_aT_b) = \delta_{ab}/2$, $[T_a, T_b] = if_{abc}T_c$ and $\{T_a, T_b\} = d_{abc}T_c$ with the structure constants f_{abc} and d_{abc}, m^2 is the meson mass parameter, c, λ_1 and λ_2 are the couplings among mesons, and ρ_i for $i = 1, 2$ are the chiral symmetry invariants $\rho_i = \mathrm{Tr}(\Phi\Phi^\dagger)^i$.

The $U_A(1)$ symmetry breaking is through the term $c\xi$ with $\xi = \det\Phi + \det\Phi^\dagger$ which mimics the $U_A(1)$ anomaly of QCD. Note that the kinetic term $\mathrm{Tr}[\partial_\mu\Phi\partial^\mu\Phi^\dagger]$ and the $U_A(1)$ breaking term preserve the $SU_L(3)\times SU_R(3)$ chiral symmetry.

The quark section $\mathcal{L}_q$ reads

$$\mathcal{L}_q = \bar{\psi}(i\gamma^\mu\partial_\mu - m_0 + \mu\gamma^0 - g\Phi_5)\psi, \tag{6}$$

where the quark-meson interaction is through the meson matrix $\Phi_5 = T^a(\sigma_a + i\gamma_5\pi_a)$ with the coupling constant g. Since we focus on the temperature behavior of the $U_A(1)$ and chiral symmetries in this work, we neglect in the following the quark chemical potential matrix μ.

The terms $\mathrm{Tr}[H(\Phi+\Phi^\dagger)]$ in $\mathcal{L}_m$ and $m_0\bar{\psi}\psi$ in $\mathcal{L}_q$ break explicitly the chiral symmetry of the system and lead to nonzero pion mass in vacuum, where the matrix H is defined as $H = h_aT_a$ with nine parameters h_a.

For the $U_A(1)$ transformation at the quark level,

$$\psi \to e^{-i\theta_A\gamma_5T^0}\psi \tag{7}$$

with the QCD vacuum angle θ_A, or

$$\psi \to \psi - i\theta_A\gamma_5\psi/\sqrt{6} \tag{8}$$

for an infinite small transformation, one has accordingly the transformation for mesons in the quark-meson model

$$\begin{aligned}\bar{\psi}_m\psi_n &\to \bar{\psi}_m\psi_n - 2\theta_A\bar{\psi}_m i\gamma_5\psi_n/\sqrt{6}, \\ \bar{\psi}_m i\gamma_5\psi_n &\to \bar{\psi}_m i\gamma_5\psi_n + 2\theta_A\bar{\psi}_m\psi_n/\sqrt{6},\end{aligned} \tag{9}$$

or

$$\begin{aligned}\sigma_a &\to \sigma_a - 2\theta_A\pi_a/\sqrt{6}, \\ \pi_a &\to \pi_a + 2\theta_A\sigma_a/\sqrt{6},\end{aligned} \tag{10}$$

which can be expressed in a compact way,

$$\Phi \to (1 + i2\theta_A/\sqrt{6})\Phi,$$
$$\det\Phi \to (1 + i\sqrt{6}\theta_A)\det\Phi. \tag{11}$$

Under the transformations (8) and (11), only the Kobayashi-Maskawa–'t Hooft (KMT) term $c\xi$ and the two explicit chiral breaking terms $m_0\bar{\psi}\psi$ and $\mathrm{Tr}[H(\Phi + \Phi^\dagger)]$ in the Lagrangian density (4) change with the variation

$$\Delta\mathcal{L} = i2\theta_A/\sqrt{6}[3c(\det\Phi - \det\Phi^\dagger) + m_0\bar{\psi}\gamma_5\psi + \mathrm{Tr}(H(\Phi - \Phi^\dagger))]. \tag{12}$$

On the other hand, according to Noether's theorem, the variation of the Lagrangian density by the $U_A(1)$ transformation can be written as

$$\begin{aligned}\Delta\mathcal{L} &= \partial_\mu\frac{\partial\mathcal{L}}{\partial(\partial_\mu\psi)}\Delta\psi + \partial_\mu\frac{\partial\mathcal{L}}{\partial(\partial_\mu\sigma_a)}\Delta\sigma_a + \partial_\mu\frac{\partial\mathcal{L}}{\partial(\partial_\mu\pi_a)}\Delta\pi_a\\ &= \partial_\mu[\bar{\psi}i\gamma^\mu\Delta\psi + \partial^\mu\sigma_a\Delta\sigma_a + \partial^\mu\pi_a\Delta\pi_a]\\ &= \partial_\mu\left[\frac{\theta_A}{\sqrt{6}}(\bar{\psi}\gamma^\mu\gamma_5\psi - 2\partial^\mu\sigma_a\pi_a + 2\partial^\mu\pi_a\sigma_a)\right],\end{aligned} \tag{13}$$

where we have used the explicit expression of the meson kinetic term

$$\mathrm{Tr}[\partial_\mu\Phi\partial^\mu\Phi^\dagger] = \frac{1}{2}(\partial_\mu\sigma_a\partial^\mu\sigma_a + \partial_\mu\pi_a\partial^\mu\pi_a). \tag{14}$$

From the comparison of (12) with (13), we have the conservation law in the quark-meson model,

$$\begin{aligned}\partial_\mu J_5^\mu &= \partial_\mu(\bar{\psi}\gamma^\mu\gamma_5\psi - 2\partial^\mu\sigma_a\pi_a + 2\partial^\mu\pi_a\sigma_a)\\ &= -12c\mathrm{Im}\det\Phi + 2im_0\bar{\psi}\gamma_5\psi + 2i\mathrm{Tr}(H(\Phi - \Phi^\dagger)).\end{aligned} \tag{15}$$

Taking the definition of the topological charge density (1) and considering the meson degrees of freedom in the quark-meson model, the above conservation law defines the charge density $Q(x)$ in the model,

$$Q(x) = -2c\mathrm{Im}\det\Phi(x). \tag{16}$$

Considering the idea that the KMT term in the quark-meson model is used to mimic the $U_A(1)$ anomaly at the hadron level, it is the only source of the topological charge density. The last two terms in (15) come from the explicit chiral symmetry breaking at the quark and hadron levels, and they are not related to the $U_A(1)$ anomaly.

With the 18 scalar and pseudoscalar mesons, the charge density can be explicitly expressed as a sum of all possible products of three meson fields,

$$\begin{aligned}Q = \frac{c}{2}\Bigg[&\sqrt{\frac{2}{27}}\pi_0^3 - \frac{1}{\sqrt{27}}\pi_8^3 - \frac{1}{\sqrt{6}}\pi_0\left(\sum_{a=1}^{8}(\pi_a^2 - \sigma_a^2) + 2\sigma_0^2\right) + \frac{1}{2}\pi_3\left(\sum_{a=4}^{5}(\pi_a^2 - \sigma_a^2) - \sum_{a=6}^{7}(\pi_a^2 - \sigma_a^2)\right)\\ &+ \frac{1}{\sqrt{3}}\pi_8\left(\sum_{a=1}^{3}(\pi_a^2 - \sigma_a^2) - \frac{1}{2}\sum_{a=4}^{7}(\pi_a^2 - \sigma_a^2) + \sigma_8^2\right) + \pi_1\left(\sum_{a=4}^{5}(\pi_a\pi_{a+2} - \sigma_a\sigma_{a+2}) + \sqrt{\frac{2}{3}}\sigma_0\sigma_1 - \frac{2}{\sqrt{3}}\sigma_1\sigma_8\right)\\ &+ \pi_2\left(\pi_5\pi_6 - \pi_4\pi_7 + \sqrt{\frac{2}{3}}\sigma_0\sigma_2 - \sigma_5\sigma_6 + \sigma_4\sigma_7 - \frac{2}{\sqrt{3}}\sigma_2\sigma_8\right) + \sqrt{\frac{2}{3}}\pi_3(\sigma_0\sigma_3 - \sqrt{2}\sigma_3\sigma_8)\\ &+ \pi_4\left(\sqrt{\frac{2}{3}}\sigma_0\sigma_4 - \sigma_3\sigma_4 - \sigma_1\sigma_6 + \sigma_2\sigma_7 + \frac{1}{\sqrt{3}}\sigma_4\sigma_8\right) + \pi_5\left(\sqrt{\frac{2}{3}}\sigma_0\sigma_5 - \sigma_3\sigma_5 - \sigma_2\sigma_6 - \sigma_1\sigma_7 + \frac{1}{\sqrt{3}}\sigma_5\sigma_8\right)\\ &- \pi_6\left(\sigma_1\sigma_4 - \sqrt{\frac{2}{3}}\sigma_0\sigma_6 - \sigma_3\sigma_6 + \sigma_2\sigma_5 - \frac{1}{\sqrt{3}}\sigma_6\sigma_8\right) + \pi_7\left(\sigma_2\sigma_4 + \sqrt{\frac{2}{3}}\sigma_0\sigma_7 - \sigma_1\sigma_5 + \sigma_3\sigma_7 + \frac{1}{\sqrt{3}}\sigma_7\sigma_8\right)\\ &+ \sqrt{\frac{2}{3}}\pi_8\sigma_0\sigma_8\Bigg].\end{aligned} \tag{17}$$

Having obtained the expression of the topological charge density $Q(x)$ in the quark-meson model, we calculate the topological susceptibility χ according to the definition (3). By separating the fields $\varphi_i = \sigma_a, \pi_a$ into the condensate and fluctuation parts $\varphi_i(x) = \langle\varphi_i\rangle + \varphi_i^{\mathrm{fl}}(x)$ and following Wick's theorem, we take a full contraction in the connected correlation function $\langle T(Q(x)Q(0))\rangle$ in terms of the meson condensates $\langle\varphi_i\rangle$ and the meson propagators $G_{ij}(x,y) = G_{ii}(x,y)\delta_{ij} = \langle\varphi_i^{\mathrm{fl}}(x)\varphi_i^{\mathrm{fl}}(y)\rangle\delta_{ij}$,

$$\chi = \left(\frac{c}{12\sqrt{6}}\right)^2 \sum_{i,j,k,l,m,n=\sigma_a,\pi_a} \int d^4x[a_{\mathrm{ijklmn}}\langle\varphi_i\rangle\langle\varphi_j\rangle G_{kl}(x,0)\langle\varphi_m\rangle\langle\varphi_n\rangle + b_{\mathrm{ijklmn}}\langle\varphi_i\rangle\langle\varphi_j\rangle G_{kl}(x,0)G_{mn}(0,0)$$
$$+ c_{\mathrm{ijklmn}}G_{ij}(x,x)G_{kl}(x,0)\langle\varphi_m\rangle\langle\varphi_n\rangle + d_{\mathrm{ijklmn}}\langle\varphi_i\rangle G_{jm}(x,0)G_{kl}(x,0)\langle\varphi_n\rangle$$
$$+ e_{\mathrm{ijklmn}}G_{ij}(x,x)G_{kl}(x,0)G_{mn}(0,0) + f_{\mathrm{ijklmn}}G_{in}(x,0)G_{jm}(x,0)G_{kl}(x,0)], \tag{18}$$

where the terms without the propagator $G(x,0)$ between the two points x and 0 are excluded from the connected correlation function. The first four terms in the square brackets, which are all with condensates, are diagrammatically shown in Fig. 1(a), and the fifth and sixth terms, which contain only closed propagators $G(x,x)$ and $G(0,0)$ and propagators $G(x,0)$ between the space-time points x and 0, are shown in Figs. 1(b) and 1(c). Since only the scalar mesons σ_0 and σ_8 can couple to vacuum without violating Lorentz invariance and parity, the classical field $\langle\varphi\rangle$ contains only two components $\langle\sigma_0\rangle$ and $\langle\sigma_8\rangle$. This largely reduces the terms in (18) and simplifies the calculation of χ.

It is clear that the four terms shown in Fig. 1(a) control the susceptibility χ in the chiral breaking phase at low temperature where the condensates are nonzero. However, the last two terms shown in Figs. 1(b) and 1(c) become dominant in the symmetry restoration phase at high temperature where the chiral condensate vanishes in the chiral limit and fluctuations characterize the system. Note that both the $U_A(1)$ breaking and the $SU(3)$ flavor breaking in the Lagrangian density (5) result in off-diagonal propagators $G_{08}(x,y)$ and $G_{80}(x,y)$, but by diagonalizing the subspace $a = 0$, 8, the off-diagonal elements disappear, and there exist only diagonal propagators $G_{ij}(x,y) = G_{ii}(x,y)\delta_{ij}$. The lowest order contribution to the correlation comes from the first diagram in Fig. 1(a), which involves four condensates and one propagator $G(x,0)$,

$$\int d^4xG_{ll}(x,0) = \frac{1}{(2\pi)^4}\int d^4xd^4pG_{ll}(p)e^{ip\cdot x} = \frac{1}{M_l^2}. \tag{19}$$

This term governs the topological susceptibility before the chiral restoration, and the temperature dependence is from

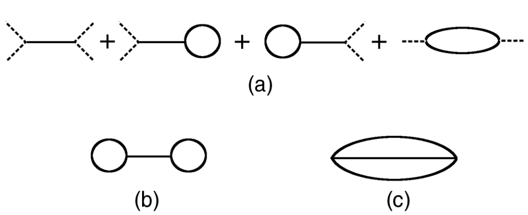

FIG. 1. Diagrammatic representation of the topological susceptibility χ with (a) and without (b),(c) explicit condensate contribution. The dashed and solid lines indicate, respectively, the meson condensates and propagators.

the condensates $\langle\sigma_0\rangle(T)$ and $\langle\sigma_8\rangle(T)$ and mass $M_l(T)$ for the meson species l, which will be calculated in the framework of the functional renormalization group in the next section.

For the closed propagators $G(x,x)$ and $G(0,0)$ shown as 1PI diagrams in Figs. 1(a) and 1(b), by doing the Matsubara frequency summation in the imaginary time formalism of finite temperature field theory, one has

$$\begin{aligned} G_{ll}(x,x) = G_{ll}(0,0) &= \int\frac{d^4p}{(2\pi)^4}\frac{i}{p^2-M_l^2} \\ &= T\int\frac{d^3\mathbf{p}}{(2\pi)^3}\sum_n\frac{1}{\omega_n^2+\epsilon_l^2} \\ &= \int\frac{d^3\mathbf{p}}{(2\pi)^3}\frac{f(\epsilon_l)}{\epsilon_l}, \end{aligned} \tag{20}$$

where $\omega_n = 2n\pi T$ with $n = 0, \pm1, \pm2, \cdots$ the boson frequencies, $f(\epsilon_l) = 1/(e^{\beta\epsilon_l}-1)$ is the Bose-Einstein distribution function with $\beta = 1/T$ and meson energy $\epsilon_l = \sqrt{\mathbf{p}^2+M_l^2}$, and we have subtracted the divergent term $1/\epsilon_l$ in the last step by a simple renormalization.

The last diagram in Fig. 1(a) includes a 2PI loop between the two condensates,

$$\begin{aligned} &\int d^4xG_{ll}(x,0)G_{mm}(x,0) \\ &= \int\frac{d^4xd^4pd^4q}{(2\pi)^8}G_{ll}(p)G_{mm}(q)e^{i(p+q)x} \\ &= T^2\int\frac{d^3\mathbf{p}d^3\mathbf{q}}{(2\pi)^3}\sum_{j,k}\frac{\beta\delta_{jk}\delta(\mathbf{p}+\mathbf{q})}{(\omega_j^2+\epsilon_l^2)(\omega_k^2+\epsilon_k^2)} \\ &= T^2\int\frac{d^3\mathbf{p}d^3\mathbf{q}}{(2\pi)^3}\sum_{j,k}\frac{(e^{i\beta\omega_j}-e^{i\beta\omega_k})\delta(\mathbf{p}+\mathbf{q})}{(i\omega_j-i\omega_k)(\omega_j^2+\epsilon_l^2)(\omega_k^2+\epsilon_m^2)} \\ &= \int\frac{d^3\mathbf{p}d^3\mathbf{q}}{(2\pi)^3}\frac{\delta(\mathbf{p}+\mathbf{q})}{\epsilon_l^2-\epsilon_m^2}\left(\frac{f(\epsilon_l)}{\epsilon_l}-\frac{f(\epsilon_m)}{\epsilon_m}\right) \end{aligned} \tag{21}$$

with the meson energies $\epsilon_l = \sqrt{\mathbf{p}^2+M_l^2}$ and $\epsilon_m = \sqrt{\mathbf{q}^2+M_m^2}$, where we have subtracted again the divergent terms in the last step.

Like Figs. 1(b) and 1(c) comes purely from the quantum fluctuations and does not depend on the condensates explicitly. With a similar technique for the Matsubara frequency summation used in (21), we have

$$\int d^4xG_{ll}(x,0)G_{mm}(x,0)G_{nn}(x,0)$$
$$=\int\frac{d^4xd^4pd^4qd^4k}{(2\pi)^{12}}G_{ll}(p)G_{mm}(q)G_{nn}(k)e^{i(p+q+k)x}$$
$$=T^3\int\frac{d^3\mathbf{p}d^3\mathbf{q}d^3\mathbf{k}}{(2\pi)^6}\sum_{i,j,k}\frac{\beta\delta_{i,j+k}\delta(\mathbf{p}+\mathbf{q}+\mathbf{k})}{(\omega_i^2+\epsilon_l^2)(\omega_j^2+\epsilon_m^2)(\omega_k^2+\epsilon_n^2)}$$
$$=\int\frac{d^3\mathbf{p}d^3\mathbf{q}d^3\mathbf{k}}{(2\pi)^6}\delta(\mathbf{p}+\mathbf{q}+\mathbf{k})$$
$$\times\sum_{ijk=lnm,mln,nml}\left[\frac{\epsilon_i^2-\epsilon_j^2-\epsilon_k^2}{(\epsilon_n^2-\epsilon_l^2-\epsilon_m^2)^2-4\epsilon_l^2\epsilon_m^2}\frac{f(\epsilon_j)f(\epsilon_k)}{\epsilon_j\epsilon_k}\right.$$
$$\left.+\frac{\epsilon_i+\epsilon_j}{(\epsilon_i+\epsilon_j)^2-\epsilon_k^2}\frac{f(\epsilon_k)}{2\epsilon_l\epsilon_m\epsilon_n}\right] \tag{22}$$

with the meson energies $\epsilon_l=\sqrt{\mathbf{p}^2+M_l^2}$, $\epsilon_m=\sqrt{\mathbf{q}^2+M_m^2}$, and $\epsilon_n=\sqrt{\mathbf{k}^2+M_n^2}$, where we have used the relationship between two distribution functions $f(\epsilon_l)f(\epsilon_m)/f(\epsilon_l+\epsilon_m)=f(\epsilon_l)+f(\epsilon_m)+1$ and again subtracted the divergent terms not accompanied by any distribution function.

The momentum integration of the three terms with two distribution functions in (22) is convergent obviously and can be simplified further. For instance, it reads

$$\int\frac{d^3\mathbf{p}^3\mathbf{q}d^3\mathbf{k}}{(2\pi)^6}\frac{\delta(\mathbf{p}+\mathbf{q}+\mathbf{k})(\epsilon_n^2-\epsilon_l^2-\epsilon_m^2)}{(\epsilon_n^2-\epsilon_l^2-\epsilon_m^2)^2-4\epsilon_l^2\epsilon_m^2}\frac{f(\epsilon_l)f(\epsilon_m)}{\epsilon_l\epsilon_m}$$
$$=\int\frac{\mathrm{dpdqpq}}{32\pi^4}\ln\left|\frac{((\epsilon_l+\epsilon_m)^2-\epsilon_n^{+2})((\epsilon_l-\epsilon_m)^2-\epsilon_n^{+2})}{((\epsilon_l+\epsilon_m)^2-\epsilon_n^{-2})((\epsilon_l-\epsilon_m)^2-\epsilon_n^{-2})}\right|$$
$$\times\frac{f(\epsilon_l)f(\epsilon_m)}{\epsilon_l\epsilon_m} \tag{23}$$

with the meson energies $\epsilon_n^+=\sqrt{(\mathbf{p}+\mathbf{q})^2+M_n^2}$ and $\epsilon_n^-=\sqrt{(\mathbf{p}-\mathbf{q})^2+M_n^2}$. The momentum integration of the other three terms with only one distribution function in (22) is divergent, and the renormalization is done in Ref. [52]. For instance, it reads

$$\int\frac{d^3\mathbf{p}d^3\mathbf{q}d^3\mathbf{k}}{(2\pi)^6}\delta(\mathbf{p}+\mathbf{q}+\mathbf{k})\frac{\epsilon_m+\epsilon_n}{(\epsilon_m+\epsilon_n)^2-\epsilon_l^2}\frac{f(\epsilon_l)}{2\epsilon_l\epsilon_m\epsilon_n}$$
$$=\frac{1}{32\pi^4}\left[-\int_0^1d\alpha\ln\left(\alpha\frac{M_m^2}{M_l^2}+(1-\alpha)\left(\frac{M_n^2}{M_l^2}-\alpha\right)\right)\right.$$
$$\left.-\gamma_E+\ln\left(4\pi\frac{\mu^2}{M_l^2}\right)\right]\int dpp^2\frac{f(\epsilon_l)}{\epsilon_l} \tag{24}$$

with the Euler constant γ_E and the factorization scale $\mu=1$ GeV.

III. QUANTIZATION WITH THE FUNCTIONAL RENORMALIZATION GROUP

We now review the application of the functional renormalization group to the $SU(3)$ quark-meson model; the details can be seen in Refs. [26,28,31,39,50]. The core quantity in the framework of the FRG is the averaged effective action Γ_k at a momentum scale k in Euclidean space. In quantum field theory, fluctuations are included in the effective action Γ by functionally integrating the classical action,

$$\Gamma[\Phi,\psi]=\int\mathcal{D}\Phi^\dagger\mathcal{D}\Phi\mathcal{D}\bar{\psi}\mathcal{D}\psi e^{-S_{cl}[\Phi,\psi]} \tag{25}$$

with $S_{cl}[\Phi,\psi]=\int d^4x\mathcal{L}(\Phi,\psi)$. However, working out this integration is almost impossible if there is any interaction involving in the Lagrangian density. As an effective way adopted in the FRG, an averaged action which is a function of the renormalization group scale k is introduced [40],

$$\Gamma_k[\Phi,\psi]=\int\mathcal{D}\Phi^\dagger\mathcal{D}\Phi\mathcal{D}\bar{\psi}\mathcal{D}\psi e^{-(S[\Phi,\psi]+\Delta S_k[\Phi,\psi])}, \tag{26}$$

where the scale dependence is carried by the additional action $\Delta S_k[\Phi,\psi]=\int d^4x[\mathrm{Tr}(\Phi^\dagger \mathrm{R_k^B}\Phi)+\bar{\psi}\mathrm{R_k^F}\psi]$, and the infrared cutoff functions R_k^B for bosons and R_k^F for fermions should be properly chosen to suppress the fluctuations at low momentum. Once k approaches zero, there would be no fluctuations suppressed. In this way, all the fluctuations are gradually included as k evolves from the ultraviolet limit to the infrared limit. Details of the evolution are coded in the flow equation for the averaged action Γ_k [40],

$$k\partial_k\Gamma_k=\frac{1}{2}\mathrm{Tr}\frac{k\partial_kR_k^B}{\Gamma_k^{B(2)}+R_k^B}-\mathrm{Tr}\frac{k\partial_kR_k^F}{\Gamma_k^{F(2)}+R_k^F}, \tag{27}$$

where $\Gamma_k^{B(2)}$ and $\Gamma_k^{F(2)}$ are second order functional derivatives of Γ_k with respect to the boson and fermion fields. In our calculation below, we choose the cutoff functions as the optimized regulators [41]

$$R_k^B(\mathbf{p})=\mathbf{p}^2\left(\frac{k^2}{\mathbf{p}^2}-1\right)\Theta\left(1-\frac{\mathbf{p}^2}{k^2}\right) \tag{28}$$

for bosons and

$$R_k^F(\mathbf{p})=i\not{\mathbf{p}}\left(\sqrt{\frac{k^2}{\mathbf{p}^2}}-1\right)\Theta\left(1-\frac{\mathbf{p}^2}{k^2}\right) \tag{29}$$

for fermions.

To solve the flow equation, we take the local potential approximation [40] which is good enough if we consider only the condensates and meson spectra. At this level, all the fluctuations are supposed to be included in an effective potential $U_k(\Phi)$, which is reduced to the classical potential

$$U_\Lambda(\langle\Phi\rangle) = m^2\langle\rho_1\rangle + \lambda_1\langle\rho_1\rangle^2 + \lambda_2\langle\rho_2\rangle - c\langle\xi\rangle - h_0\langle\sigma_0\rangle - h_8\langle\sigma_8\rangle \tag{30}$$

at the ultraviolet limit $k = \Lambda$ where all the fluctuations are supposed to vanish. Assuming homogeneous condensates and after doing directly the momentum integration and Matsubara frequency summation at finite temperature, the flow equation (27) is simplified as a partial differential equation for the effective potential [50],

$$\partial_k U_k(\langle\Phi\rangle) = \frac{k^4}{12\pi^2}\left[\sum_b \frac{1}{E_b}\coth\frac{E_b}{2T} - 12\sum_f \frac{1}{E_f}\tanh\frac{E_f}{2T}\right] \tag{31}$$

with 18 boson and three fermion energies $E_b = \sqrt{k^2+M_b^2}$, $(b=\pi_a,\sigma_a)$, and $E_f = \sqrt{k^2+M_f^2}$, $(f = u, d, s)$.

The two independent condensates $\langle\sigma_0\rangle$ and $\langle\sigma_8\rangle$ or the light (chiral) and strange condensates $\langle\sigma_u\rangle = \sqrt{\frac{2}{3}}\langle\sigma_0\rangle + \sqrt{\frac{1}{3}}\langle\sigma_8\rangle$ and $\langle\sigma_s\rangle = \sqrt{\frac{1}{3}}\langle\sigma_0\rangle - \sqrt{\frac{2}{3}}\langle\sigma_8\rangle$ are determined by the minimization of the potential,

$$\frac{\partial U_k(\langle\Phi\rangle)}{\partial\langle\sigma_u\rangle} = \frac{\partial U_k(\langle\Phi\rangle)}{\partial\langle\sigma_s\rangle} = 0. \tag{32}$$

This leads to the scale dependence of the condensates $\langle\sigma_u\rangle_k$ and $\langle\sigma_s\rangle_k$. The dynamical quark and meson masses are defined as the coefficients of the quadratic terms $\bar\psi\psi$, $\pi_a^{\rm fl}\pi_b^{\rm fl}$, and $\sigma_a^{\rm fl}\sigma_b^{\rm fl}$ in the Lagrangian density after the separations $\pi_a = \langle\pi_a\rangle + \pi_a^{\rm fl}$ and $\sigma_a = \langle\sigma_a\rangle + \sigma_a^{\rm fl}$,

$$\begin{aligned} M_u = M_d &= m_0 + \frac{1}{2}g\langle\sigma_u\rangle_k, \\ M_s &= m_0 + \frac{1}{\sqrt{2}}g\langle\sigma_s\rangle_k, \\ (M_S^2)_{ab} &= \left.\frac{\partial^2 U_k(\Phi)}{\partial\sigma_a\partial\sigma_b}\right|_{\Phi\to\langle\Phi\rangle}, \\ (M_P^2)_{ab} &= \left.\frac{\partial^2 U_k(\Phi)}{\partial\pi_a\partial\pi_b}\right|_{\Phi\to\langle\Phi\rangle}. \end{aligned} \tag{33}$$

The meson masses are just the eigenvalues of the curvature of the effective potential $U_k(\Phi)$. They form two 9×9 matrices M_S^2 and M_P^2, and seven of their diagonal elements are the masses of the scalar mesons a_0 and κ and pseudoscalar mesons π and K. Because of the $U_A(1)$ breaking and the $SU(3)$ flavor breaking, there exists one independent nonzero off-diagonal element for each matrix, $(M_S^2)_{08} = (M_S^2)_{80}$ and $(M_P^2)_{08} = (M_P^2)_{80}$. Diagonalizing the meson subspace $a = 0, 8$ generates the pseudoscalar mesons η and η' and the corresponding scalar mesons which are the eigenstates of the Hamiltonian of the model [2,39],

$$\begin{aligned} \eta_0 &= \cos\theta_P\eta - \sin\theta_P\eta', \\ \eta_8 &= \sin\theta_P\eta + \cos\theta_P\eta', \end{aligned} \tag{34}$$

where θ_P is the mixing angle in the pseudoscalar channel and can be expressed in terms of the masses,

$$\tan 2\theta_P = \frac{2(M_P^2)_{08}}{(M_P^2)_{00} - (M_P^2)_{88}}. \tag{35}$$

Note that the definition of the mixing angle (34) is different from the often used one; see, for instance, Ref. [11]. While these definitions are different, the idea of using the mixing angle as a measure of $U_A(1)$ breaking is kept in any definition, and the difference does not affect the topological susceptibility χ, since it depends only on the condensates and meson masses; see (18)–(24).

In the chiral limit, it is reduced to

$$\tan 2\theta_P = 2\sqrt{2} \tag{36}$$

in the chiral restoration phase, which leads to a constant mixing angle $\theta \simeq 35^0$ after the phase transition. In a real case, we expand the angle in powers of the chiral condensate $\langle\sigma_u\rangle$ at high temperature where chiral symmetry is partially restored and $\langle\sigma_u\rangle$ becomes small,

$$\tan 2\theta_P = 2\sqrt{2}\left(1 - \frac{9\langle\sigma_u\rangle}{2((M_S^2)_{11} - (M_S^2)_{44})}\right) + \mathcal{O}(\langle\sigma_u\rangle^2), \tag{37}$$

where the strange condensate $\langle\sigma_s\rangle$ hides in the scalar meson masses in the denominator, and the relation between the masses and the light condensate $(M_P^2)_{00} - (M_P^2)_{88} \sim (M_S^2)_{11} - (M_S^2)_{44} + \mathcal{O}(\langle\sigma_u\rangle)$ is used. For the scalar channel, we can introduce the mixing angle θ_S in a similar way. In the chiral limit, there is no mixing $\theta_S = 0$ in the chiral symmetry restoration phase due to $(M_S^2)_{08} = 0$.

It is necessary to note that we can analytically prove the Goldstone theorem corresponding to the spontaneous chiral symmetry breaking in the FRG frame.

IV. NUMERICAL RESULTS

We now numerically solve the flow equation (31) for the effective potential U_k together with the gap equations for the condensates $\langle\sigma_u\rangle$ and $\langle\sigma_s\rangle$. Both sides of the flow equation depend only on $\langle\sigma_u\rangle$ and $\langle\sigma_s\rangle$ or $\langle\rho_1\rangle$ and $\langle\rho_2\rangle$; it is then a first order differential equation with initial condition $U_{k=\Lambda}$ at the ultraviolet limit, and we can numerically solve the effective potential as a whole in a two-dimensional grid [28]. The evolution of the potential is evaluated by discretizing the potential in the plane of $\langle\rho_1\rangle$ and $\langle\rho_2\rangle$. We also adopt the clamped cubic splines to evaluate the derivatives of the potential with respect to $\langle\rho_1\rangle$ and $\langle\rho_2\rangle$ and interpolate the potential in order to find the global minimum.

We first solve the flow equation in vacuum. We choose the ultraviolet momentum $\Lambda = 1$ GeV which is the typical scale of effective models at the hadron level. The initial potential U_Λ is so chosen to fit the pseudoscalar meson masses M_π, M_K, M_η, and $M_{\eta'}$, decay constants f_π and f_K, and dynamical quark mass or chiral condensate $\langle\sigma_u\rangle$ in vacuum. For our calculation in the real case, we take the renormalization parameters $m_\Lambda^2 = (867.76\ \mathrm{MeV})^2$, $\lambda_{1\Lambda} = -32/3$, and $\lambda_{2\Lambda} = 50$, the $U_A(1)$ breaking parameter $c = 4807.84$ MeV, the chiral breaking parameters $h_u = 2(120.73\ \mathrm{MeV})^2$ and $h_s = \sqrt{2}(336.41\ \mathrm{MeV})^2$, and the Yukawa coupling strength $g = 6.5$. Considering the fact that the system at high enough momentum is dominated by the dynamics and not affected remarkably by the temperature, the temperature dependence of the initial condition of the flow equation at the ultraviolet momentum can be safely neglected. Therefore, we take the temperature-independent initial condition $U_\Lambda(T) = U_\Lambda$ in vacuum.

We now show the temperature dependence of the condensates in Fig. 2. In the chiral limit with $h_u = 0$, the light condensate $\langle\sigma_u\rangle$, which is the order parameter of the chiral phase transition, continuously drops with temperature and goes to zero at the critical temperature $T_c = 140$ MeV. In the real case with nonzero h_u, the chiral phase transition becomes a crossover, and the order parameter decreases very rapidly around the critical temperature. The temperature dependence of the strange condensate $\langle\sigma_s\rangle$ is rather smooth in comparison with the light condensate; it decreases with temperature gradually and is nonzero in the symmetry restoration phase.

The masses of the nine scalar mesons σ, κ, f_0 and a_0 and nine pseudoscalar mesons π, K, η, and η' are shown in Fig. 3 as functions of temperature. In the chiral limit, π's are the three Goldstone modes, their mass is maintained at zero in the chiral breaking phase. At the critical point, σ becomes also massless. In the symmetry restoration phase, it is easy to find $(M_S^2)_{00} = (M_P^2)_{11}$ and $(M_S^2)_{44} = (M_P^2)_{44}$, which means the degeneration of π's and σ and K's and κ's. In the real case, the degeneration disappears, but the corresponding scalar and pseudoscalar mesons approach each other at high temperature. While the η and η' mass splitting becomes much weaker in the chiral restoration phase than in the symmetry breaking phase, it does not vanish. This indicates $U_A(1)$ symmetry breaking even at extremely high temperature.

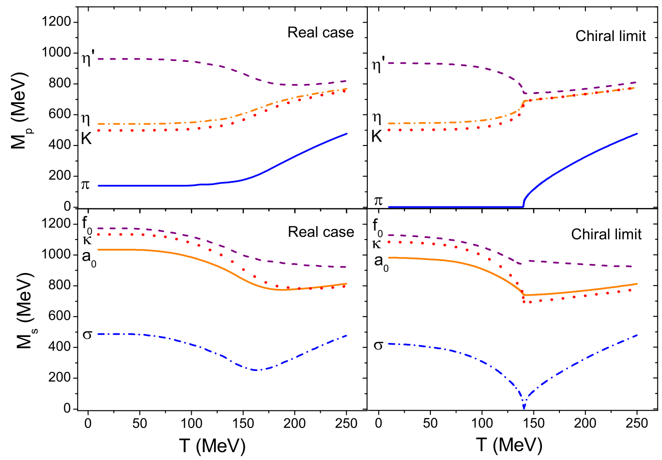

FIG. 3. The scalar and pseudoscalar meson masses M_S and M_P as functions of temperature in the chiral limit (right panel) and real case (left panel).

Figure 4 shows the mixing angles θ_P and θ_S as functions of temperature in the chiral limit and real case. At $T = 0$, the angles are determined by the meson masses in vacuum. In the chiral limit, the pseudoscalar angle increases with temperature from the starting value $\theta_P \simeq -5°$, then crosses zero and jumps up suddenly at the critical point of the chiral

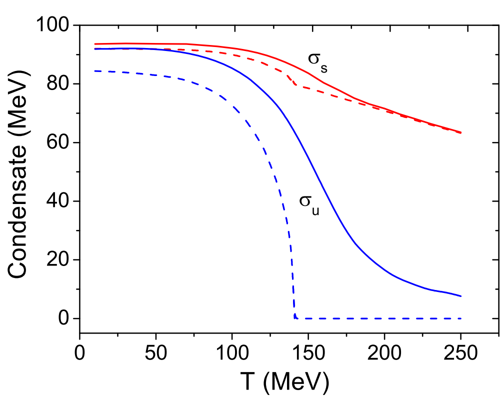

FIG. 2. The light and strange condensates $\langle\sigma_u\rangle/2$ and $\langle\sigma_s\rangle/\sqrt{2}$ as functions of temperature in the chiral limit (dashed lines) and real case (solid lines).

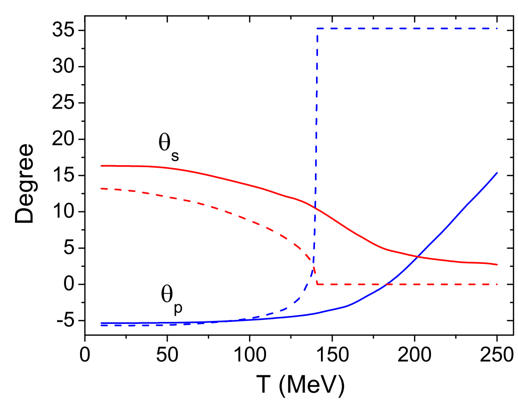

FIG. 4. The pseudoscalar and scalar mixing angles θ_P and θ_S as functions of temperature in the chiral limit (dashed lines) and real case (solid lines).

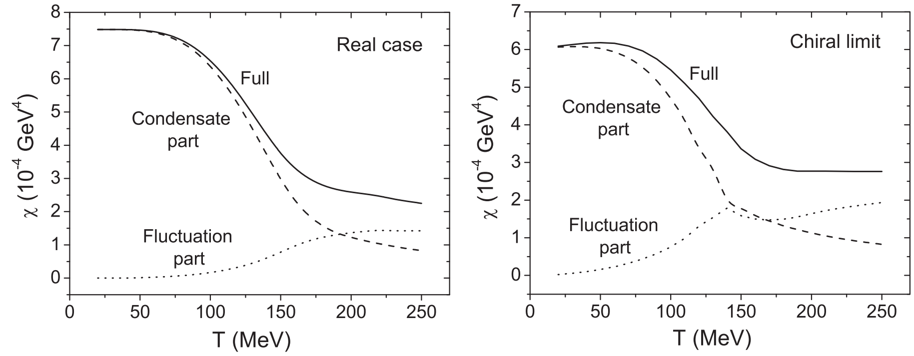

FIG. 5. The topological susceptibility χ as a function of temperature in the chiral limit (left panel) and real case (right panel). Dashed and dotted lines are the contributions controlled by the condensates and fluctuations, respectively, and solid lines are the full results.

phase transition, and finally keeps as a constant $\theta_P \simeq 35°$ in the symmetry restoration phase, as we analyzed in the last section. In the real case, the sudden jump disappears, and the angle gradually approaches 35° in the high temperature limit. The temperature behavior of the scalar angle θ_S is very similar to the chiral condensate $\langle\sigma_u\rangle$. In contrast with θ_P, it drops continuously with increasing temperature. In the chiral restoration phase, it disappears in the chiral limit and is still sizeable in the real case.

Now we come to the topological susceptibility χ, which is the most straightforward criterion for the quantum anomaly. From its expression shown in Eq. (18) or Fig. 1, it contains the condensate-dominated part and the fluctuation-induced part indicated, respectively, by dashed and dotted lines in Fig. 5. Using the known condensates $\langle\sigma_u\rangle$ and $\langle\sigma_s\rangle$ and the meson mass matrices M_S^2 and M_P^2 with off-diagonal elements $(M_S^2)_{08}$, $(M_S^2)_{80}$, $(M_P^2)_{08}$, and $(M_P^2)_{80}$, we can directly calculate the susceptibility by summarizing all six-field correlations in (18). An alternative way is to diagonalize the subspace with $a = 0$, 8 and use the 18 scalar and pseudoscalar eigenstates of the model and the mixing angels θ_S and θ_P. The two calculations are equivalent. In both the chiral limit case and real case, while the condensates control the susceptibility in the chiral symmetry breaking phase, and around the critical point, the fluctuations become the dominant contribution at high temperature. Different from the condensate-controlled part, which drops continuously with increasing temperature, the fluctuation-induced part goes up with temperature. As a result, there will be still $U_A(1)$ symmetry breaking in the chiral symmetry restoration phase.

Since the KMT term introduced in the meson section of the quark-meson model is used to effectively describe the topological charge (2) induced by the gluon fields of QCD, the topological susceptibility calculated here is an analogy to the Yang-Mills topological susceptibility χ_{YM} [10–12]. However, we took some approximations in our calculations. For instance, we considered only meson condensates and propagators in (18) and neglected the contribution from all the higher correlations. Therefore, as an effective χ calculated at the hadron level, it can be considered as an approximation of the lattice simulated χ_{YM}. What we want to emphasize in this paper is the importance of the fluctuations. Without the fluctuations, it is impossible to correctly describe the behavior of the $U_A(1)$ breaking at high temperatures.

V. CONCLUSION

We investigated the $U_A(1)$ symmetry and its relation to the chiral symmetry at finite temperature by applying the functional renormalization group to the $SU(3)$ quark-meson model. We calculated the mass gap and mixing angel between η and η' mesons and the topological susceptibility to see if the $U_A(1)$ symmetry is restored at high temperature. Since the mass gap and mixing angle are defined through meson masses at the mean-field level, the former approaches zero and the latter becomes a constant in the chiral symmetry restoration phase. This means that the two symmetries are restored at almost the same critical temperature. However, this is the conclusion in mean-field approximation. When the fluctuations are included in the calculation of the topological susceptibility, which is the most straightforward criterion for the anomaly, the conclusion is very different. The susceptibility contains two parts, the condensate-controlled part, which behaves like the mass gap and mixing angle, and the fluctuation-induced part, which becomes dominant in the chiral restoration phase. The former drops and the latter goes up with increasing temperature. As a result of the competition, the full susceptibility is still remarkably large when the chiral symmetry is restored. It is necessary to note that our discussion here on $U_A(1)$ and chiral symmetries is in the scope of hadrons. Beyond the scope, the quantum and thermal fluctuations at the meson level will break down due to meson melting in a hot medium, and the susceptibility should finally disappear at extremely high temperature because of the nontrivial gluon configurations fading out.

ACKNOWLEDGMENTS

The work is supported by the NSFC and MOST Grants No. 11335005, No. 11575093, No. 2013CB922000, and No. 2014CB845400.

[1] G. 't Hooft, Phys. Rev. D **14**, 3432 (1976); **18**, 2199(E) (1978).
[2] H. Leutwyler and A. V. Smilga, Phys. Rev. D **46**, 5607 (1992).
[3] E. Witten, Nucl. Phys. **B156**, 269 (1979).
[4] G. Veneziano, Nucl. Phys. **B159**, 213 (1979).
[5] C. Rosenzweig, J. Schechter, and C. G. Trahern, Phys. Rev. D **21**, 3388 (1980).
[6] T. Schafer, Phys. Lett. B **389**, 445 (1996).
[7] K. Kawarabayashi and N. Ohta, Nucl. Phys. **B175**, 477 (1980).
[8] K. Kawarabayashi and N. Ohta, Prog. Theor. Phys. **66**, 1789 (1981).
[9] R. Alkofer, arXiv:1102.3166.
[10] S. Benic, D. Horvatic, D. Kekez, and D. Klabucar, Phys. Rev. D **84**, 016006 (2011).
[11] S. Benic, D. Horvatic, D. Kekez, and D. Klabucar, Phys. Lett. B **738**, 113 (2014).
[12] V. Bernard, S. Descotes-Genon, and G. Toucas, J. High Energy Phys. 06 (2012) 051.
[13] D. Horvatic, D. Klabucar, and A. E. Radzhabov, Phys. Rev. D **76**, 096009 (2007).
[14] B. Alles, M. D'Elia, and A. Di Giacomo, Nucl. Phys. **B494**, 281 (1997); **B679**, 397(E) (2004).
[15] B. Alles, M. D'Elia, A. Di Giacomo, and P. W. Stephenson, Nucl. Phys. B, Proc. Suppl. **73**, 518 (1999).
[16] O. Wantz and E. P. S. Shellard, Nucl. Phys. **B829**, 110 (2010).
[17] A. Bazavov, T. Bhattacharya, M. Buchoff, M. Cheng, N. Christ, H. Ding, R. Gupta, P. Hegde, C. Jung, F. Karsch, Z. Lin, R. Mawhinney, S. Mukherjee, P. Petreczky, R. Soltz, P. Vranas, and H. Yin, Phys. Rev. D **86**, 094503 (2012).
[18] G. Cossu, S. Aoki, H. Fukaya, S. Hashimoto, T. Kaneko, H. Matsufuru, and J. Noaki, Phys. Rev. D **87**, 114514 (2013).
[19] Y. Nambu and G. Jona-Lasinio, Phys. Rev. **122**, 345 (1961).
[20] U. Vogl and W. Weise, Prog. Part. Nucl. Phys. **27**, 195 (1991).
[21] S. Klevansky, Rev. Mod. Phys. **64**, 649 (1992).
[22] M. Volkov, Phys. Part. Nucl. **24**, 35 (1993).
[23] T. Hatsuda and T. Kunihiro, Phys. Rep. **247**, 221 (1994).
[24] M. Buballa, Phys. Rep. **407**, 205 (2005).
[25] M. Gell-Mann and M. Levy, Nuovo Cimento **16**, 705 (1960).
[26] J. T. Lenaghan, D. H. Rischke, and J. Schaffner-Bielich, Phys. Rev. D **62**, 085008 (2000).
[27] S. Gasiorowicz and D. Geffen, Rev. Mod. Phys. **41**, 531 (1969).
[28] M. Mitter and B. J. Schaefer, Phys. Rev. D **89**, 054027 (2014).
[29] P. Zhuang, J. Hufner, and S. Klevansky, Nucl. Phys. **A576**, 525 (1994).
[30] N. Bilic and H. Nikolic, Eur. Phys. J. C **6**, 515 (1999).
[31] J. Schaffner-Bielich, Phys. Rev. Lett. **84**, 3261 (2000).
[32] K. Fukushima, K. Ohnishi, and K. Ohta, Phys. Rev. C **63**, 045203 (2001).
[33] D. Toublan and J. Kogut, Phys. Lett. B **564**, 212 (2003).
[34] A. Barducci, R. Casalbuoni, G. Pettini, and L. Ravagli, Phys. Rev. D **69**, 096004 (2004).
[35] D. Ebert and K. Klimenko, Eur. Phys. J. C **46**, 771 (2006).
[36] H. Mao, N. Petropoulos, and W. Zhao, J. Phys. G **32**, 2187 (2006).
[37] H. Abuki, R. Anglani, R. Gatto, M. Pellicoro, and M. Ruggieri, Phys. Rev. D **79**, 034032 (2009).
[38] J. Andersen and L. Kyllingstad, J. Phys. G **37**, 015003 (2010).
[39] B. Schaefer and M. Wagner, Phys. Rev. D **79**, 014018 (2009).
[40] J. Berges, arXiv:hep-ph/9902419; H. Gies, Lect. Notes Phys. **852**, 287 (2012); P. Kopietz, L. Bartosch, and F. Schutz, Lect. Notes Phys. **798**, 1 (2010).
[41] D. F. Litim, Phys. Rev. D **64**, 105007 (2001); G. Papp, B. J. Schaefer, H. J. Pirner, and J. Wambach, Phys. Rev. D **61**, 096002 (2000).
[42] S. Floerchinger, R. Schmidt, S. Moroz, and C. Wetterich, Phys. Rev. A **79**, 013603 (2009).
[43] B. Friman, K. Hebeler, and A. Schwenk, Lect. Notes Phys. **852**, 245 (2012).
[44] T. K. Herbst, J. M. Pawlowski, and B. J. Schaefer, Phys. Lett. B **696**, 58 (2011).
[45] B. Stokic, B. Friman, and K. Redlich, Eur. Phys. J. C **67**, 425 (2010).
[46] O. Bohr, B. J. Schaefer, and J. Wambach, Int. J. Mod. Phys. A **16**, 3823 (2001).
[47] J. P. Blaizot, A. Ipp, R. Mendez-Galain, and N. Wschebor, Nucl. Phys. **A784**, 376 (2007).
[48] B. J. Schaefer and H. J. Pirner, Nucl. Phys. **A660**, 439 (1999).
[49] K. Fukushima, K. Kamikado, and B. Klein, Phys. Rev. D **83**, 116005 (2011).
[50] Y. Jiang and P. Zhuang, Phys. Rev. D **86**, 105016 (2012).
[51] T. Xia, L. He, and P. Zhuang, Phys. Rev. D **88**, 056013 (2013).
[52] J. Baacke and S. Michalski, Phys. Rev. D **67**, 085006 (2003).